Journal of Computational Physics 231 (2012) 3007–3022

Contents lists available at SciVerse ScienceDirect

Journal of Computational Physics

journal homepage: www.elsevier.com/locate/jcp

An efficient and stable spectral method for electromagnetic scattering from a layered periodic structure

Ying He [a], David P. Nicholls [b], Jie Shen [a,*]

[a] Department of Mathematics, Purdue University, West Lafayette, IN 47907, United States
[b] Department of Mathematics, Statistics and Computer Science, University of Illinois at Chicago, Chicago, IL 60607, United States

ARTICLE INFO

Article history:
Received 2 May 2011
Received in revised form 25 October 2011
Accepted 28 October 2011
Available online 9 November 2011

Keywords:
Electromagnetic scattering
Boundary perturbation methods
High-order spectral methods
Transmission boundary conditions

ABSTRACT

The scattering of acoustic and electromagnetic waves by periodic structures plays an important role in a wide range of problems of scientific and technological interest. This contribution focuses upon the stable and high-order numerical simulation of the interaction of time-harmonic electromagnetic waves incident upon a periodic doubly layered dielectric media with sharp, irregular interface. We describe a boundary perturbation method for this problem which avoids not only the need for specialized quadrature rules but also the dense linear systems characteristic of boundary integral/element methods. Additionally, it is a provably stable algorithm as opposed to other boundary perturbation approaches such as Bruno and Reitich's "method of field expansions" or Milder's "method of operator expansions". Our spectrally accurate approach is a natural extension of the "method of transformed field expansions" originally described by Nicholls and Reitich (and later refined to other geometries by the authors) in the single-layer case.

1. Introduction

The interaction of acoustic and electromagnetic waves with periodic structures plays an important role in a wide range of problems of scientific and technological interest. From grating couplers [7,8,30] to nanostructures [17] to remote sensing [29], the ability to simulate in a robust and accurate way the fields generated by such structures is of crucial importance to researchers from many disciplines. In this contribution we focus upon the stable and high-order numerical simulation of the interaction of time-harmonic electromagnetic waves incident upon a periodic doubly layered dielectric material with sharp, irregular interface. While we focus on the simplified model of a two-dimensional structure, the core of the algorithm will remain the same for a fully three-dimensional simulation governed by the full Maxwell's equations.

In this work we describe a boundary perturbation method (BPM) for the numerical simulation of scattering returns from an irregularly shaped, periodic, doubly layered medium. We focus upon periodic structures as they arise from a large number of engineering applications, however, this choice does simplify our numerical approach (e.g. we may use the discrete Fourier transform to approximate Fourier coefficients). However, we note that this simplification is also realized for competing methods as well. For such problems *surface* methods are preferred as a discretization of the interface alone significantly reduces the number of unknowns to be recovered. However, such methods face a number of drawbacks.

One compelling choice is a surface integral method [6] (e.g. boundary integral methods—BIM—or boundary element methods—BEM) which only requires a discretization of the layer *interface* (rather than the whole structure) and which, due to the choice of the Green's function, enforces the far-field boundary condition exactly. While this method can deliver

* Corresponding author.
E-mail address: shen@math.purdue.edu (J. Shen).

0021-9991/$ - see front matter © 2011 Elsevier Inc. All rights reserved.
doi:10.1016/j.jcp.2011.10.033

high-accuracy simulations with greatly reduced operation counts, there are several difficulties which need to be addressed. First, high-order simulations can only be realized with specially designed quadrature rules which respect the singularities in the Green's function (and its derivative, in certain formulations). Additionally, BIM/BEM typically give rise to dense linear systems to be solved which require carefully designed preconditioned iterative methods (with accelerated matrix-vector products, e.g. by the fast-multipole method [10]) for configurations of engineering interest.

An alternative to a BIM/BEM is a boundary perturbation method and two popular approaches are the "method of field expansions" (FE) due to Bruno and Reitich [3–5] and the "method of operator expansions" (OE) of Milder [11–16]. These methods are very appealing as they posit *surface* unknowns thereby enjoying the favorable operation counts of surface integral methods, while avoiding the subtle quadrature rules, dense linear systems, and required matrix-vector product accelerations described above. However, Nicholls and Reitich showed that these algorithms depend upon strong cancellations (e.g. differences of extremely large quantities to produce order one results) for their convergence which results in ill-conditioned numerics. We refer the interested reader to [19–21] for a full description of these phenomena.

In addition to these results, Nicholls and Reitich described an alternative boundary perturbation algorithm, the "method of transformed field expansions" (TFE), which does *not* rely on strong cancellations for its convergence. In fact, the resulting recursions can be used for a *direct*, *rigorous* demonstration of the strong convergence of the relevant perturbation expansions in an appropriate function space. Furthermore, these formulas were implemented to reveal a stable and highly accurate numerical scheme for the simulation of scattering returns by periodic gratings. This work was generalized by the authors to the case of irregular bounded obstacles in two [18] and three dimensions [9], and even resulted in a rigorous numerical analysis of the method [28,22]. In this contribution, we construct a highly non-trivial extension to the case of periodic gratings separating two materials of different dielectric constants. Here, of course, one must be concerned not only with a reflected field and its far-field boundary condition, but also with a transmitted field which satisfies a different condition at infinity.

The organization of the paper is as follows: In Section 2 we recall the governing equations of an electromagnetic field incident upon a periodic, two-dimensional irregular grating. In Section 3 we define a change of variables which significantly enhances the conditioning properties of our numerical scheme resulting in the "method of transformed field expansions." We discuss a Legendre–Galerkin method to solve the resulting two-point boundary value problem in Section 4 and present extensive numerical results in Section 5.

2. Governing equations

We consider the problem of simulating the scattering of electromagnetic waves in a layered periodic structure. More precisely, we consider two domains

$$\Omega^+ := \{y > g(x)\}, \quad \Omega^- := \{y < g(x)\},$$

where $y = g(x)$ is the shape of the d-periodic interface (see Fig. 1). These regions are filled with materials of dielectric constants ϵ^+ and ϵ^-, respectively. The permeability in each domain is assumed to be μ_0, that of the vacuum.

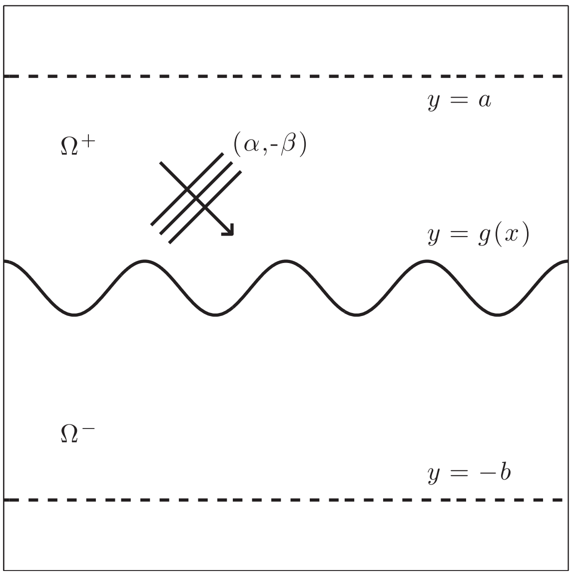

Fig. 1. Geometric illustration of the problem.

The grating is illuminated by time-harmonic plane-wave radiation

$$\widetilde{\mathbf{E}}^{\mathbf{i}} = \mathbf{A}e^{i\alpha x - i\beta y}e^{-i\omega t}, \quad \widetilde{\mathbf{H}}^{\mathbf{i}} = \mathbf{B}e^{i\alpha x - i\beta y}e^{-i\omega t},$$

which will be scattered both above and below the surface. This gives rise to reduced total fields

$$\begin{aligned} &\mathbf{E} = \mathbf{E}^{\mathbf{i}} + \mathbf{E}^{+}, \quad \mathbf{H} = \mathbf{H}^{\mathbf{i}} + \mathbf{H}^{+}, \quad y > g(x), \\ &\mathbf{E} = \mathbf{E}^{-}, \quad \mathbf{H} = \mathbf{H}^{-}, \quad y < g(x), \end{aligned}$$

where, e.g.

$$\mathbf{E} = \mathbf{E}(x,y) := \widetilde{\mathbf{E}}(x,y,t)e^{i\omega t}, \quad \mathbf{H} = \mathbf{H}(x,y) := \widetilde{\mathbf{H}}(x,y,t)e^{i\omega t},$$

if $\{\widetilde{\mathbf{E}}, \widetilde{\mathbf{H}}\}$ are the unreduced, time dependent fields. The incident, reflected, refracted, and total electric and magnetic fields all satisfy the time-harmonic Maxwell's equations:

$$\nabla \times \mathbf{E} = i\omega\mu_0\mathbf{H}, \quad \mathrm{div}[\mathbf{E}] = 0, \tag{2.1a}$$

$$\nabla \times \mathbf{H} = -i\omega\epsilon\mathbf{E}, \quad \mathrm{div}[\mathbf{H}] = 0, \tag{2.1b}$$

where $\epsilon = \epsilon^{\pm}$ depending upon the domain of definition [6]. At the grating surface the total fields satisfy the transmission conditions

$$N \times (\mathbf{E}^{\mathbf{i}} + \mathbf{E}^{+} - \mathbf{E}^{-}) = 0, \quad N \times (\mathbf{H}^{\mathbf{i}} + \mathbf{H}^{+} - \mathbf{H}^{-}) = 0, \tag{2.2}$$

where $N = (-\partial_x g(x), 0, 1)^T$ is a normal vector. Finally, the periodicity of the grating enforces the *quasi-periodicity* of the fields

$$\mathbf{E}(x+d,y) = e^{i\alpha d}\mathbf{E}(x,y), \quad \mathbf{H}(x+d,y) = e^{i\alpha d}\mathbf{H}(x,y),$$

and the scattered waves must be *outgoing*.

It is not difficult to show that if both the grating shape and incident radiation are independent of z then so are $\mathbf{E}$ and $\mathbf{H}$ [24]. In this case the time-harmonic Maxwell's Eqs. (2.1) reduce to the Helmholtz equation

$$\Delta u + (k^{\pm})^2 u = 0,$$

where $k^{\pm} := \omega\sqrt{\mu_0\epsilon^{\pm}}$, and $u = u(x,y)$ is either $E^{\pm,3}$ (transverse electric—TE—component) or $H^{\pm,3}$ (transverse magnetic—TM—component). Furthermore, the z-components of the conditions in (2.2) read

$$0 = E^3 = E^{+,3} + E^{i,3} - E^{-,3}$$

and

$$0 = \partial_N E^3 = [\partial_y - (\partial_x g)\partial_x](E^3) = [\partial_y - (\partial_x g)\partial_x](E^{+,3} + E^{i,3} - E^{-,3}).$$

Writing in coordinates and simplifying we find

$$\begin{aligned} &u^{+}(x,g(x)) - u^{-}(x,g(x)) = -e^{i\alpha x - i\beta g(x)}, \\ &\partial_N u^{+}(x,g(x)) - \sigma^2\partial_N u^{-}(x,g(x)) = ((i\beta) + (i\alpha)\partial_x g(x))e^{i\alpha x - i\beta g(x)}, \end{aligned}$$

where $\sigma^2 = 1$ for the TE mode, while

$$\sigma^2 = \frac{\epsilon^{+}}{\epsilon^{-}} = \left(\frac{k^{+}}{k^{-}}\right)^2,$$

for the TM mode. Thus, the governing equations we consider are

$$\Delta u^{+} + (k^{+})^2 u^{+} = 0, \quad y > g(x), \tag{2.3a}$$

$$\mathrm{OWC}[u^{+}] = 0, \quad y \to \infty, \tag{2.3b}$$

$$\Delta u^{-} + (k^{-})^2 u^{-} = 0, \quad y < g(x) \tag{2.3c}$$

$$\mathrm{OWC}[u^{-}] = 0, \quad y \to -\infty, \tag{2.3d}$$

$$u^{+} - u^{-} = -\phi(x), \quad y = g(x), \tag{2.3e}$$

$$\partial_N u^{+} - \partial_N u^{-} = ((i\beta) + (i\alpha)\partial_x g(x))\phi(x), \quad y = g(x), \tag{2.3f}$$

$$u^{\pm}(x+d,y) = e^{i\alpha d}u^{\pm}(x,y), \tag{2.3g}$$

where

$$\phi(x) := e^{i\alpha x - i\beta g(x)} \tag{2.3h}$$

and we make the "outgoing wave condition" (OWC) operators more precise presently.

For the far-field boundary conditions consider the hyperplanes $\{y = a\}$, $\{y = -b\}$ where $a, b > |g|_{L^\infty}$. The augmented system of governing equations

$$\Delta u^+ + (k^+)^2 u^+ = 0, \quad g(x) < y < a, \tag{2.4a}$$
$$\partial_y u^+ = \partial_y v^+, \quad y = a, \tag{2.4b}$$
$$u^+ = v^+, \quad y = a, \tag{2.4c}$$
$$\Delta v^+ + (k^+)^2 v^+ = 0, \quad y > a, \tag{2.4d}$$
$$\mathrm{OWC}[v^+] = 0, \quad y \to \infty, \tag{2.4e}$$
$$\Delta u^- + (k^-)^2 u^- = 0, \quad -b < y < g(x), \tag{2.4f}$$
$$\partial_y u^- = \partial_y v^-, \quad y = -b, \tag{2.4g}$$
$$u^- = v^-, \quad y = -b, \tag{2.4h}$$
$$\Delta v^- + (k^-)^2 v^- = 0, \quad y < -b, \tag{2.4i}$$
$$\mathrm{OWC}[v^-] = 0, \quad y \to -\infty, \tag{2.4j}$$
$$u^+ - u^- = -\phi(x), \quad y = g(x), \tag{2.4k}$$
$$\partial_N u^+ - \partial_N u^- = ((i\beta) + (i\alpha)\partial_x g(x))\phi(x), \quad y = g(x), \tag{2.4l}$$
$$u^\pm(x + d, y) = e^{i\alpha d} u^\pm(x, y), \tag{2.4m}$$
$$v^\pm(x + d, y) = e^{i\alpha d} v^\pm(x, y), \tag{2.4n}$$

are equivalent to (2.3). To make the far–field boundary condition more precise we note that solutions of (2.4d) and (2.4e) are

$$v^+(x, y) = \sum_{p=-\infty}^{\infty} \hat{\psi}_p e^{i\alpha_p x + i\beta_p^+ (y-a)},$$

where

$$\alpha_p := \alpha + (2\pi/d)p, \quad \beta_p^\pm := \begin{cases} \sqrt{(k^\pm)^2 - \alpha_p^2} & p \in U^\pm \\ i\sqrt{\alpha_p^2 - (k^\pm)^2} & p \notin U^\pm \end{cases},$$

$$U^\pm := \{p \in \mathbf{Z} \mid (k^\pm)^2 - \alpha_p^2 > 0\},$$

$\mathbf{Z}$ are the integers, and

$$\psi(x) := u^+(x, a) = \sum_{p=-\infty}^{\infty} \hat{\psi}_p e^{i\alpha_p x}.$$

Similarly, solutions of (2.4i) and (2.4j) are

$$v^-(x, y) = \sum_{p=-\infty}^{\infty} \hat{\zeta}_p e^{i\alpha_p x - i\beta_p^- (y+b)},$$

where

$$\zeta(x) := u^-(x, -b) = \sum_{p=-\infty}^{\infty} \hat{\zeta}_p e^{i\alpha_p x}.$$

To close the set of equations for u^+ we simply need to produce $\partial_y v^+$ in (2.4b):

$$\partial_y v^+(x, a) = \sum_{p=-\infty}^{\infty} \left(i\beta_p^+\right) \hat{\psi}_p e^{i\alpha_p x} =: T^+[\psi] = T^+[u^+(x, a)].$$

A similar analysis at $y = -b$ yields an operator

$$T^-[\zeta] := \sum_{p=-\infty}^{\infty} (-i\beta_p^-) \hat{\zeta}_p e^{i\alpha_p x},$$

and the system (2.4) can be *equivalently* restated as

$$\Delta u^+ + (k^+)^2 u^+ = 0, \quad g(x) < y < a, \tag{2.5a}$$
$$\partial_y u^+ - T^+[u^+] = 0, \quad y = a, \tag{2.5b}$$
$$\Delta u^- + (k^-)^2 u^- = 0, \quad -b < y < g(x), \tag{2.5c}$$
$$\partial_y u^- - T^-[u^-] = 0, \quad y = -b, \tag{2.5d}$$
$$u^+ - u^- = -\phi(x), \quad y = g(x), \tag{2.5e}$$
$$\partial_N u^+ - \partial_N u^- = ((i\beta) + (i\alpha)\partial_x g(x))\phi(x), \quad y = g(x), \tag{2.5f}$$
$$u^\pm(x+d, y) = e^{i\alpha d} u^\pm(x, y). \tag{2.5g}$$

3. Transformed field expansion

As has been demonstrated in previous publications on boundary perturbation algorithms for electromagnetic scattering [19–21], the transformed field expansion (TFE) method can dramatically improve the conditioning of the resulting recursions. The TFE method consists of two essential steps: (i) "domain flattening" through a simple change of variables; and (ii) boundary perturbation. We now describe the two steps in detail.

3.1. Change of variables

We define

$$x' = x,$$
$$y' = a\left(\frac{y-g}{a-g}\right), \quad g < y < a,$$
$$y'' = b\left(\frac{y-g}{b+g}\right), \quad -b < y < g,$$

which gives rise to the differentiation rules:

$$(a-g)\partial_x = (a-g)\partial_{x'} - (\partial_{x'} g)(a-y')\partial_{y'},$$
$$(a-g)\partial_y = a\partial_{y'},$$

for $g(x) < y < a$, and

$$(b+g)\partial_x = (b+g)\partial_{x'} - (\partial_{x'} g)(b+y'')\partial_{y''},$$
$$(b+g)\partial_y = b\partial_{y''},$$

for $-b < y < g(x)$. With this change of variables (2.5) becomes

$$\left(\partial_{x'}^2 + \partial_{y'}^2\right)u^+(x',y') + (k^+)^2 u^+(x',y') = F^+(x',y'), \quad 0 < y' < a, \tag{3.1a}$$
$$\partial_{y'} u^+(x',a) - T^+[u^+(x',a)] = J^+(x'), \tag{3.1b}$$
$$\left(\partial_{x'}^2 + \partial_{y''}^2\right)u^-(x',y'') + (k^-)^2 u^-(x',y'') = F^-(x',y''), \quad -b < y'' < 0, \tag{3.1c}$$
$$\partial_{y''} u^-(x',-b) - T^-[u^-(x',-b)] = J^-(x'), \tag{3.1d}$$
$$u^+(x',0) - u^-(x',0) = -\phi(x'), \tag{3.1e}$$
$$\partial_{y'} u^+(x',0) - \partial_{y''} u^-(x',0) = Q(x',0). \tag{3.1f}$$

In these equations

$$F^\pm(x',y') = \partial_{x'} F_x^\pm(x',y') + \partial_{y'} F_y^\pm(x',y') + F_h^\pm(x',y'), \tag{3.1g}$$

where

$$F_x^+ = \frac{2}{a} g \partial_{x'} u^+ - \frac{1}{a^2} g^2 \partial_{x'} u^+ + \frac{a-y'}{a}(\partial_{x'} g)\partial_{y'} u^+ - \frac{a-y'}{a^2} g(\partial_{x'} g)\partial_{y'} u^+, \tag{3.1h}$$
$$F_y^+ = \frac{a-y'}{a}(\partial_{x'} g)\partial_{x'} u^+ - \frac{a-y'}{a^2} g(\partial_{x'} g)\partial_{x'} u^+ - \frac{(a-y')^2}{a^2}(\partial_{x'} g)^2 \partial_{y'} u^+, \tag{3.1i}$$

and

$$F_h^+ = -\frac{1}{a}(\partial_{x'} g)\partial_{x'} u^+ + \frac{1}{a^2} g(\partial_{x'} g)\partial_{x'} u^+ + \frac{a-y'}{a^2}(\partial_{x'} g)^2 \partial_{y'} u^+ + (k^+)^2 \frac{2}{a} g u^+ - (k^+)^2 \frac{1}{a^2} g^2 u^+, \tag{3.1j}$$

and

$$F_x^- = -\frac{2}{b} g \partial_{x'} u^- - \frac{1}{b^2} g^2 \partial_{x'} u^- + \frac{b+Y''}{b} (\partial_{x'} g) \partial_{Y''} u^- + \frac{b+Y''}{b^2} g (\partial_{x'} g) \partial_{Y''} u^-, \tag{3.1k}$$

$$F_y^- = \frac{b+Y''}{b} (\partial_{x'} g) \partial_{x'} u^- + \frac{b+Y''}{b^2} g (\partial_{x'} g) \partial_{x'} u^- - \frac{(b+Y'')^2}{b^2} (\partial_{x'} g)^2 \partial_{Y''} u^-, \tag{3.1l}$$

and

$$F_h^- = \frac{1}{b} (\partial_{x'} g) \partial_{x'} u^- + \frac{1}{b^2} g (\partial_{x'} g) \partial_{x'} u^- - \frac{b+Y''}{b^2} (\partial_{x'} g)^2 \partial_{Y''} u^- - (k^-)^2 \frac{2}{b} g u^- - (k^-)^2 \frac{1}{b^2} g^2 u^-. \tag{3.1m}$$

Furthermore,

$$J^+ = -\frac{1}{a} g T^+[u^+], \tag{3.1n}$$

$$J^- = \frac{1}{b} g T^-[u^-], \tag{3.1o}$$

and

$$Q = \frac{1}{ab} \{ (ab + ag - bg - g^2)(i\alpha \partial_{x'} g + i\beta)\phi(x') - ag \partial_{y'} u^+ + (\partial_{x'} g)(b+g)(a-g) \partial_{x'} u^+ \\ -(\partial_{x'} g)^2 a (b+g) \partial_{y'} u^+ - bg \partial_{y''} u^- - (\partial_{x'} g)(b+g)(a-g) \partial_{x'} u^- + (\partial_{x'} g)^2 b (a-g) \partial_{y''} u^- \}. \tag{3.1p}$$

3.2. Recursion by boundary perturbation

We shall now describe a boundary perturbation algorithm to solve the transformed system (3.1). If we let $g = \varepsilon f$ and f is sufficiently smooth, the transformed fields can be shown to be analytic. Hence, we can write

$$u^\pm(x, y; \varepsilon) = \sum_{n=0}^{\infty} u_n^\pm(x, y) \varepsilon^n.$$

Inserting the above into (3.1), it is straightforward, albeit tedious, to derive the following recursions for u_n:

$$\left(\partial_{x'}^2 + \partial_{y'}^2\right) u_n^+(x', y') + (k^+)^2 u_n^+(x', y') = F_n^+(x', y'), \quad 0 < y' < a, \tag{3.2a}$$

$$\partial_{y'} u_n^+(x', a) - T^+[u_n^+(x', a)] = J_n^+(x'), \tag{3.2b}$$

$$\left(\partial_{x'}^2 + \partial_{y''}^2\right) u_n^-(x', y'') + (k^-)^2 u_n^-(x', y'') = F_n^-(x', y''), \quad -b < y'' < 0, \tag{3.2c}$$

$$\partial_{y''} u_n^-(x', -b) - T^-[u_n^-(x', -b)] = J_n^-(x'), \tag{3.2d}$$

$$u_n^+(x', 0) - u_n^-(x', 0) = \phi_n(x'), \tag{3.2e}$$

$$\partial_{y'} u_n^+(x', 0) - \partial_{y''} u_n^-(x', 0) = Q_n(x', 0). \tag{3.2f}$$

In these equations

$$F_n^\pm(x', y') = \partial_{x'} F_{n,x}^\pm(x', y') + \partial_{y'} F_{n,y}^\pm(x', y') + F_{n,h}^\pm(x', y'), \tag{3.2g}$$

where

$$F_{n,x}^+ = \frac{2}{a} f \partial_{x'} u_{n-1}^+ - \frac{1}{a^2} f^2 \partial_{x'} u_{n-2}^+ + \frac{a-y'}{a} (\partial_{x'} f) \partial_{y'} u_{n-1}^+ - \frac{a-y'}{a^2} f (\partial_{x'} f) \partial_{y'} u_{n-2}^+, \tag{3.2h}$$

$$F_{n,y}^+ = \frac{a-y'}{a} (\partial_{x'} f) \partial_{x'} u_{n-1}^+ - \frac{a-y'}{a^2} f (\partial_{x'} f) \partial_{x'} u_{n-2}^+ - \frac{(a-y')^2}{a^2} (\partial_{x'} f)^2 \partial_{y'} u_{n-2}^+, \tag{3.2i}$$

and

$$F_{n,h}^+ = -\frac{1}{a} (\partial_{x'} f) \partial_{x'} u_{n-1}^+ + \frac{1}{a^2} f (\partial_{x'} f) \partial_{x'} u_{n-2}^+ + \frac{a-y'}{a^2} (\partial_{x'} f)^2 \partial_{y'} u_{n-2}^+ + (k^+)^2 \frac{2}{a} f u_{n-1}^+ - (k^+)^2 \frac{1}{a^2} f^2 u_{n-2}^+, \tag{3.2j}$$

and

$$F_{n,x}^- = -\frac{2}{b} f \partial_{x'} u_{n-1}^- - \frac{1}{b^2} f^2 \partial_{x'} u_{n-2}^- + \frac{b+Y''}{b} (\partial_{x'} f) \partial_{Y''} u_{n-1}^- + \frac{b+Y''}{b^2} f (\partial_{x'} f) \partial_{Y''} u_{n-2}^-, \tag{3.2k}$$

$$F_{n,y}^- = \frac{b+Y''}{b} (\partial_{x'} f) \partial_{x'} u_{n-1}^- + \frac{b+Y''}{b^2} f (\partial_{x'} f) \partial_{x'} u_{n-2}^- - \frac{(b+Y'')^2}{b^2} (\partial_{x'} f)^2 \partial_{Y''} u_{n-2}^-, \tag{3.2l}$$

and

$$F^-_{n,h} = \frac{1}{b}(\partial_{x'} f)\partial_{x'} u^-_{n-1} + \frac{1}{b^2} f(\partial_{x'} f)\partial_{x'} u^-_{n-2} - \frac{b+Y''}{b^2}(\partial_{x'} f)^2 \partial_{Y''} u^-_{n-2} - (k^-)^2 \frac{2}{b} f u^-_{n-1} - (k^-)^2 \frac{1}{b^2} f^2 u^-_{n-2}. \tag{3.2m}$$

Furthermore,

$$J^+_n = -\frac{1}{a} f T^+[u^+_{n-1}], \tag{3.2n}$$

$$J^-_n = \frac{1}{b} f T^-[u^-_{n-1}], \tag{3.2o}$$

$$\phi_n = (-1)^{n+1} \frac{(i\beta f)^n}{n!} e^{i\alpha x}, \tag{3.2p}$$

and

$$\begin{aligned} Q_n = \frac{1}{ab}\Big\{ & -iab\beta\phi_n - iab\alpha\partial_{x'} f\phi_{n-1} - i\beta(a-b)f\phi_{n-1} - i\alpha(a-b)f\partial_{x'} f\phi_{n-2} + i\beta f^2\phi_{n-2} + i\alpha\partial_{x'} f f^2\phi_{n-3} \\ & -af\partial_{y'} u^+_{n-1} + ab\partial_{x'} f\partial_{x'} u^+_{n-1} + (a-b)f\partial_{x'} f\partial_{x'} u^+_{n-2} - \partial_{x'} f f^2 \partial_{x'} u^+_{n-3} - ab(\partial_{x'} f)^2\partial_{y'} u^+_{n-2} - a(\partial_{x'} f)^2 f\partial_{y'} u^+_{n-3} \\ & -bf\partial_{y''} u^-_{n-1} - ab\partial_{x'} f\partial_{x'} u^-_{n-1} - (a-b)f\partial_{x'} f\partial_{x'} u^-_{n-2} + \partial_{x'} f f^2\partial_{x'} u^-_{n-3} + ab(\partial_{x'} f)^2\partial_{y''} u^-_{n-2} - bf(\partial_{x'} f)^2\partial_{y''} u^-_{n-3}\Big\}. \end{aligned} \tag{3.2q}$$

If we write

$$u^\pm_n(x,y) = \sum_{p=-\infty}^{\infty} u^\pm_{n,p}(y)e^{i\alpha_p x}, \quad F^\pm_n(x,y) = \sum_{p=-\infty}^{\infty} F^\pm_{n,p}(y)e^{i\alpha_p x}, \quad J^\pm_n(x) = \sum_{p=-\infty}^{\infty} J^\pm_{n,p} e^{i\alpha_p x},$$

$$\phi_n(x) = \sum_{p=-\infty}^{\infty} \phi_{n,p} e^{i\alpha_p x}, \quad Q_n(x) = \sum_{p=-\infty}^{\infty} Q_{n,p} e^{i\alpha_p x},$$

and insert into (3.2), then we obtain a sequence of equations for $u^\pm_{n,p}(y)$:

$$\begin{aligned} &\partial^2_{y'} u^+_{n,p}(y') + \left((k^+)^2 - \alpha_p^2\right)u^+_{n,p}(y') = F^+_{n,p}, \quad 0 < y' < a, \\ &\partial^2_{y''} u^-_{n,p}(y'') + \left((k^-)^2 - \alpha_p^2\right)u^-_{n,p}(y'') = F^-_{n,p}, \quad -b < y'' < 0, \\ &\partial_{y'} u^+_{n,p}(a) - i\beta^+_p u^+_{n,p}(a) = J^+_{n,p}, \\ &\partial_{y''} u^-_{n,p}(-b) + i\beta^-_p u^-_{n,p}(-b) = J^-_{n,p}, \\ &u^+_{n,p}(0) - u^-_{n,p}(0) = \phi_{n,p}, \\ &\partial_{y'} u^+_{n,p}(0) - \partial_{y''} u^-_{n,p}(0) = Q_{n,p}. \end{aligned}$$

Due to the quasi-periodic boundary conditions we seek solutions of the form

$$u^\pm(x,y) = \sum_{n=0}^{\infty} \sum_{p=-\infty}^{\infty} u^\pm_{n,p}(y)e^{i\alpha_p x}\varepsilon^n,$$

resulting in the generic one-dimensional problem

$$\partial^2_y u^+_{p,n}(y) + ((k^+)^2 - \tilde{\alpha}^2)u^+_{p,n}(y) = F^+_{p,n}(y), \quad 0 < y < a, \tag{3.3a}$$

$$\partial^2_y u^-_{p,n}(y) + ((k^-)^2 - \tilde{\alpha}^2)u^-_{p,n}(y) = F^-_{p,n}(y), \quad -b < y < 0, \tag{3.3b}$$

$$\partial_y u^+_{p,n}(a) - i\beta^+ u^+_{p,n}(a) = J^+_{p,n}, \tag{3.3c}$$

$$\partial_y u^-_{p,n}(-b) + i\beta^- u^-_{p,n}(-b) = J^-_{p,n}, \tag{3.3d}$$

$$u^+_{p,n}(0) - u^-_{p,n}(0) = \phi_{p,n}, \tag{3.3e}$$

$$\partial_y u^+_{p,n}(0) - \partial_y u^-_{p,n}(0) = Q_{p,n}, \tag{3.3f}$$

where we have dropped the primes for convenience and denote

$$\beta^+ = \beta^+_p, \quad \beta^- = \beta^-_p, \quad \tilde{\alpha} = \alpha_p.$$

4. Legendre–Galerkin approximation

In this section we provide algorithm details of a Legendre–Galerkin approach to approximate solutions of the two-point boundary value problem (3.3). The approximation of this problem is the final specification we must make in our TFE approach to the doubly layered scattering problem at hand.

4.1. Weak formulation

Assume that $u^{*,+}(y)$ and $u^{*,-}(y)$ satisfy the following homogeneous version of (3.3):

$$\partial_y^2 u^{*,+} + ((k^+)^2 - \tilde{\alpha}^2)u^{*,+} = 0, \quad 0 < y < a, \tag{4.1a}$$

$$\partial_y^2 u^{*,-} + ((k^-)^2 - \tilde{\alpha}^2)u^{*,-} = 0, \quad -b < y < 0, \tag{4.1b}$$

$$\partial_y u^{*,+}(a) - i\beta^+ u^{*,+}(a) = J^+, \tag{4.1c}$$

$$\partial_y u^{*,-}(-b) + i\beta^- u^{*,-}(-b) = J^-, \tag{4.1d}$$

$$u^{*,+}(0) - u^{*,-}(0) = \phi, \tag{4.1e}$$

$$\partial_y u^{*,+}(0) - \partial_y u^{*,-}(0) = Q, \tag{4.1f}$$

where, for convenience, we have dropped the (n,p) subscripts. The functions

$$u^{*,+}(y) = Ae^{i\beta^+ y} + Be^{-i\beta^+ y}, \quad u^{*,-}(y) = Ce^{i\beta^- y} + De^{-i\beta^- y},$$

are solutions of (4.1a) and (4.1b), respectively, for any choices of the constants A, B, C, D. Substituting these forms into (4.1c)–(4.1f) we find A, B, C, D:

$$B = \frac{iJ^+ e^{i\beta^+ a}}{2\beta^+}, \quad C = -\frac{iJ^- e^{i\beta^- b}}{2\beta^-},$$
$$A = \frac{\beta^-(2C + \phi) + B(\beta^+ - \beta^-) - iQ}{\beta^- + \beta^+}, \quad D = \frac{\beta^+(2B - \phi) + C(\beta^- - \beta^+) - iQ}{\beta^- + \beta^+}.$$

Now consider the functions

$$\hat{u}^+(y) := u^+(y) - u^{*,+}(y), \quad \hat{u}^-(y) := u^-(y) - u^{*,-}(y),$$

where, $\hat{u}^+$ and $\hat{u}^-$ satisfy the version of (3.3) with homogeneous boundary conditions

$$\partial_y^2 \hat{u}^+(y) + ((k^+)^2 - \tilde{\alpha}^2)\hat{u}^+(y) = \widehat{F}^+, \quad 0 < y < a, \tag{4.2a}$$

$$\partial_y^2 \hat{u}^-(y) + ((k^-)^2 - \tilde{\alpha}^2)\hat{u}^-(y) = \widehat{F}^-, \quad -b < y < 0, \tag{4.2b}$$

$$\partial_y \hat{u}^+(a) - i\beta^+ \hat{u}^+(a) = 0, \tag{4.2c}$$

$$\partial_y \hat{u}^-(-b) + i\beta^- \hat{u}^-(-b) = 0, \tag{4.2d}$$

$$\hat{u}^+(0) - \hat{u}^-(0) = 0, \tag{4.2e}$$

$$\partial_y \hat{u}^+(0) - \partial_y \hat{u}^-(0) = 0. \tag{4.2f}$$

Setting

$$u(y) := \begin{cases} \hat{u}^+(y) & 0 < y < a \\ \hat{u}^-(y) & -b < y < 0 \end{cases}, \quad f(y) := \begin{cases} \widehat{F}^+(y) & 0 < y < a \\ \widehat{F}^-(y) & -b < y < 0 \end{cases},$$

$$k(y) := \begin{cases} (k^+)^2 - \tilde{\alpha}^2 & 0 < y < a \\ (k^-)^2 - \tilde{\alpha}^2 & -b < y < 0 \end{cases},$$

we find that u satisfies:

$$\partial_y^2 u(y) + k(y)^2 u(y) = f, \quad -b < y < a, \tag{4.3a}$$

$$\partial_y u(a) - i\beta^+ u(a) = 0, \tag{4.3b}$$

$$\partial_y u(-b) + i\beta^- u(-b) = 0, \tag{4.3c}$$

$$u(0^+) - u(0^-) = 0, \tag{4.3d}$$

$$\partial_y u(0^+) - \partial_y u(0^-) = 0. \tag{4.3e}$$

Denoting the Sobolev space of complex functions:

$$H^1(-b,a) := \{u, \partial_y u \in L^2(-b,a)\},$$

we define the inner product on the interval $(-b,a)$

$$(u, v) := \int_{-b}^{a} u\bar{v}dy,$$

for any u, $v \in L^2(-b,a)$ where $\bar{v}$ is the complex conjugate of v. To simplify notation, we use from here the usual notation for spaces of real functions (e.g. H^1, P_N, etc.) to denote spaces of complex functions.

With this notation the weak formulation for (4.3) is: Find $u \in H^1(-b,a)$ such that:

$$(k^2u,\phi) - (\partial_y u, \partial_y \phi) = (f,\phi) - i\beta^+ u(a)\bar{\phi}(a) - i\beta^- u(-b)\bar{\phi}(-b), \quad \forall \phi \in H^1(-b,a). \tag{4.4}$$

4.2. The Legendre–Galerkin method

Let P_N be the polynomial space of degree at most N and define

$$X_{N,\beta,\gamma} := \{u \in C(-b,a) | u|_{(0,a)}, u|_{(-b,0)} \in P_N, (\partial_y u - i\beta u)(a) = (\partial_y u + i\gamma u)(-b) = 0\}.$$

Then our Legendre–Galerkin method is to find $u_N \in X_{N,\beta^+,\beta^-}$ such that

$$(k^2u_N,\phi_N) - (\partial_y u_N, \partial_y \phi_N) = (\widetilde{I}_N f,\phi_N) - i\beta^+ u_N(a)\bar{\phi}_N(a) - i\beta^- u_N(-b)\bar{\phi}_N(-b), \quad \forall \phi \in X_{N,\beta^+,\beta^-}, \tag{4.5}$$

where $\widetilde{I}_N$ is the interpolation operator defined by $\widetilde{I}_N f|_{(0,a)}, \widetilde{I}_N f|_{(-b,0)} \in P_N$. Since every function in X_{N,β^+,β^-} is differentiable at everywhere except at zero, (4.5) is equivalent to

$$(k^2u_N,\phi_N) + (\partial_y^2 u_N,\phi_N)_{I_1} + \left(\partial_y^2 u_N,\phi_N\right)_{I_2} + [\partial_y u_N(0^+) - \partial_y u_N(0^-)]\bar{\phi}_N(0) = (\widetilde{I}_N f,\phi_N), \quad \forall \phi \in X_{N,\beta^+,\beta^-}, \tag{4.6}$$

where the subscripts I_1 and I_2 denote the corresponding integration domain $I_1 = (0,a)$ and $I_2 = (-b,0)$.

Consider $\xi^+(y) = c_1 y + 1$ and $\xi^-(y) = c_2 y + 1$ such that

$$(\partial_y \xi^+ - i\beta^+\xi^+)(a) = 0, \quad (\partial_y \xi^- + i\beta^-\xi^-)(-b) = 0.$$

It is easy to see that

$$c_1 = \frac{i\beta^+}{1 - i\beta^+ a}, \quad c_2 = \frac{-i\beta^-}{1 - i\beta^- b}.$$

Let $L_j(y)$ be the Legendre polynomial of order j on $-1 < y < 1$. Following [25] (or see [26,27]), we define

$$\varphi_j(y) := (1+i)L_j\left(\frac{2y-a}{a}\right) + a_j L_{j+1}\left(\frac{2y-a}{a}\right) + b_j L_{j+2}\left(\frac{2y-a}{a}\right), \quad j = 0,1,\ldots,N-2,$$

with the complex parameters a_j, b_j chosen such that φ_j satisfies the boundary conditions

$$(\partial_y \varphi_j - i\beta^+\varphi_j)(a) = 0, \quad \varphi_j(0) = 0.$$

Similarly, we define

$$\psi_j(y) := (1+i)L_j\left(\frac{b+2y}{b}\right) + a_j' L_{j+1}\left(\frac{b+2y}{b}\right) + b_j' L_{j+2}\left(\frac{b+2y}{b}\right), \quad j = 0,1,\ldots,N-2,$$

with a_j', b_j' selected such that ψ_j satisfies the boundary conditions

$$(\partial_y \psi_j + i\beta^-\psi_j)(-b) = 0, \quad \psi_j(0) = 0.$$

If we let

$$\tilde{\phi}_j(y) := \begin{cases} \phi_j(y), & 0 < y < a, \\ 0, & -b < y < 0, \end{cases} \quad j = 0,\ldots,N-2,$$

$$\tilde{\phi}_{N-1+j}(y) := \begin{cases} 0, & 0 < y < a, \\ \psi_j(y), & -b < y < 0, \end{cases} \quad j = 0,\ldots,N-2,$$

$$\tilde{\phi}_{2N-2}(y) := \begin{cases} \xi^+(y), & 0 < y < a, \\ \xi^-(y), & -b < y < 0 \end{cases}.$$

Then, we have

$$X_{N,\beta^+,\beta^-} = \mathrm{span}\{\tilde{\phi}_0, \tilde{\phi}_1, \ldots, \tilde{\phi}_{2N-2}\}.$$

We assume that the approximate solution has the form

$$u^N(y) := \sum_{j=0}^{2N-2} \hat{u}_j \tilde{\phi}_j(y), \tag{4.7}$$

and define

$$\hat{u} = (\hat{u}_0, \ldots, \hat{u}_{N-2})^T,$$
$$\hat{w} = (\hat{u}_{N-1}, \ldots, \hat{u}_{2N-3})^T,$$
$$\hat{f} = (\hat{f}_0, \ldots, \hat{f}_{N-2})^T,$$
$$\hat{g} = (\hat{f}_{N-1}, \ldots, \hat{f}_{2N-3})^T,$$

where

$$\hat{f}_j := (\widetilde{I}_N f, \tilde{\phi}_j), \quad j = 0, 1, \ldots, 2N-2.$$

We further define

$$s^1_{lj} = \left(\partial^2_y \tilde{\phi}_j, \tilde{\phi}_l\right)_{I_1},$$
$$s^2_{lj} = \left(\partial^2_y \tilde{\phi}_{N-1+j}, \tilde{\phi}_{N-1+l}\right)_{I_2},$$
$$m^1_{lj} = (\tilde{\phi}_j, \tilde{\phi}_l)_{I_1},$$
$$m^2_{lj} = (\tilde{\phi}_{N-1+j}, \tilde{\phi}_{N-1+l})_{I_2},$$

for $l, j = 0,1,\ldots,N-2$. Additionally, we set

$$S_1 = \left(s^1_{lj}\right), \quad S_2 = \left(s^2_{lj}\right), \quad M_1 = \left(m^1_{lj}\right), \quad M_2 = \left(m^2_{lj}\right),$$
$$a_{12}(j) = \left(\partial^2_y \tilde{\phi}_j + k^2 \tilde{\phi}_j, \tilde{\phi}_{2N-2}\right)_{I_1} + \partial_y \tilde{\phi}_j(0^+),$$
$$b_{12}(j) = \left(\partial^2_y \tilde{\phi}_{N-1+j} + k^2 \tilde{\phi}_{N-1+j}, \tilde{\phi}_{2N-2}\right)_{I_2} - \partial_y \tilde{\phi}_{N-1+j}(0^-),$$
$$a_{21}(j) = \left(\partial^2_y \tilde{\phi}_{2N-2} + k^2 \tilde{\phi}_{2N-2}, \tilde{\phi}_j\right)_{I_1},$$
$$b_{21}(j) = \left(\partial^2_y \tilde{\phi}_{2N-2} + k^2 \tilde{\phi}_{2N-2}, \tilde{\phi}_{N-1+j}\right)_{I_2},$$
$$a_{22}(j) = (k^2 \tilde{\phi}_{2N-2}, \tilde{\phi}_{2N-2}) + \partial_y \tilde{\phi}_{2N-2}(0^+) - \partial_y \tilde{\phi}_{2N-2}(0^-),$$
$$A_{11} = S_1 + (k^+)^2 M_1, \quad B_{11} = S_2 + (k^-)^2 M_2,$$

for $l, j = 0,1,\ldots,N-2$. The entries of the above matrices can be obtained exactly by using the orthogonal properties of Legendre polynomials. Upon insertion of (4.7) into (4.5) we find the following system of $2N-1$ equations:

$$\begin{pmatrix} A_{11} & 0 & a_{12} \\ 0 & B_{11} & b_{12} \\ a^T_{21} & b^T_{21} & a_{22} \end{pmatrix} \begin{pmatrix} \hat{u} \\ \hat{w} \\ \hat{u}_{2N-2} \end{pmatrix} = \begin{pmatrix} \hat{f} \\ \hat{g} \\ \hat{f}_{2N-2} \end{pmatrix}. \tag{4.8}$$

To solve this system of equations, we perform a simple block Gaussian elimination to get the following equation for $\hat{u}_{2N-2}$:

$$\left\{ a_{22} - \begin{pmatrix} a^T_{21} & b^T_{21} \end{pmatrix} \begin{pmatrix} A_{11} & 0 \\ 0 & B_{11} \end{pmatrix}^{-1} \begin{pmatrix} a_{12} \\ b_{12} \end{pmatrix} \right\} \hat{u}_{2N-2} = \hat{f}_{2N-2} - \begin{pmatrix} a^T_{21} & b^T_{21} \end{pmatrix} \begin{pmatrix} A_{11} & 0 \\ 0 & B_{11} \end{pmatrix}^{-1} \begin{pmatrix} \hat{f} \\ \hat{g} \end{pmatrix}.$$

Then, we can solve for $\hat{u}$ and $\hat{w}$ independently as follows:

$$A_{11}\hat{u} = \hat{f} - \hat{u}_{2N-2} \cdot (a_{12}),$$

and

$$B_{11}\hat{w} = \hat{g} - \hat{u}_{2N-2} \cdot b_{12}.$$

Due to the basis we chose, A_{11} and B_{11} are penta-diagonal symmetric matrices so that the above equations can be efficiently solved.

Finally, our numerical solution has the form

$$u^{N,N_x,N_y}(x,y) = \sum_{n=0}^{N} \sum_{p=-N_x/2}^{N_x/2-1} u^{N_y}_{n,p}(y) e^{i\alpha_p x} \varepsilon^n, \tag{4.9}$$

where

$$u^{N_y}_{n,p}(y) = u^*_{n,p}(y) + \sum_{j=0}^{2N_y-2} \hat{u}_{n,p,j} \tilde{\phi}_j(y)$$

with $u^*_{n,p}(y)$ from (4.1) and the $\hat{u}_{n,p,j}$ from the algorithm above using the Legendre–Galerkin approximation.

Remark 4.1. Before leaving our description of the numerical procedure, we mention that there are a number of choices for summing the Taylor series which appear in (4.9). To avoid an avalanche of impenetrable notation we focus on the generic problem of approximating the analytic function

$$A(\varepsilon) = \sum_{n=0}^{\infty} A_n \varepsilon^n$$

by its truncated Taylor series

$$A^N(\varepsilon) := \sum_{n=0}^{N} A_n \varepsilon^n.$$

It is a classic result that if ε_0 is in the disk of convergence of $A(\varepsilon)$, say $\{|\varepsilon| < \rho\}$, $A^N(\varepsilon_0)$ will converge to $A(\varepsilon_0)$ exponentially fast as $N \to \infty$. However, it is possible for ε_0 to be a point of analyticity *outside* the disk of convergence of the Taylor series and for A^N to produce meaningless results. The classical numerical analytic continuation technique of Padé approximation [1] has been successfully brought to bear upon boundary perturbation methods in the past (see, e.g. [4,21]) and we utilize this here as well. In short, Padé approximation seeks to simulate the truncated Taylor series A^N by the rational function

$$[L/M](\varepsilon) := \frac{a^L(\varepsilon)}{b^M(\varepsilon)} = \frac{\sum_{l=0}^{L} a_l \varepsilon^l}{1 + \sum_{m=1}^{M} b_m \varepsilon^m}$$

where $L + M = N$ and

$$[L/M](\varepsilon) = A^N(\varepsilon) + \mathcal{O}(\varepsilon^{L+M+1});$$

well-known formulas for the coefficients $\{a_l, b_m\}$ can be found in [1]. This approximant has the remarkable properties that, for a wide class of functions, not only is the convergence of $[L/M]$ to A at $\varepsilon = \varepsilon_0$ *faster* than that of A^N for $|\varepsilon_0| < \rho$, but also that $[L/M]$ may converge to A for points of analyticity ε_0 for which $|\varepsilon_0| > \rho$. We refer the interested reader to Section 2.2 of Baker and Graves-Morris [1] and the insightful calculations of Section 8.3 of Bender and Orszag [2] for a thorough discussion of the capabilities and limitations of Padé approximants.

5. Numerical results and discussion

We now present the results of numerical experiments which exhibit the stability and accuracy of our new algorithm. We use as a measure of convergence the widely-accepted "energy defect" [23,3–5] and study the performance of our algorithm in assorted limits of both the physical and numerical parameters.

5.1. Energy defect

To diagnose the convergence of our algorithm we appeal to the well-established energy conservation measure. We point out that *outside* the grooves, i.e. in the domain

$$\Omega_0 := \{y > |g|_{L^\infty}\} \bigcup \{y < -|g|_{L^\infty}\},$$

the solutions $u^\pm$ can be expressed via the Rayleigh expansions

$$u^+(x,y) = \sum_{p=-\infty}^{\infty} B_p^+ e^{i\alpha_p x + i\beta_p^+ y}, \quad u^-(x,y) = \sum_{p=-\infty}^{\infty} B_p^- e^{i\alpha_p x - i\beta_p^- y}. \tag{5.1}$$

In the case of real wavenumbers $k^\pm$ there is a principle of conservation of energy [23] for the TE mode which can be expressed as

$$\sum_{p\in U^+} \beta_p^+ |B_p^+|^2 + \sum_{p\in U^-} \beta_p^- |B_p^-|^2 = \beta_0^+.$$

Defining the energy

$$E^\pm(l) := \mathrm{Im}\left\{\frac{1}{L}\int_0^L \overline{u^\pm}(x,l)(\partial_y u^\pm(x,l))dx\right\}, \tag{5.2}$$

we have the following relationship:

Lemma 5.1. *If $l_1 > |g|_{L^\infty}$ and $l_2 < -|g|_{L^\infty}$ then*

$$E^+(l_1) - E^-(l_2) = \sum_{p\in U^+} \beta_p^+ |B_p^+|^2 + \sum_{p\in U^-} \beta_p^- |B_p^-|^2 = \beta_0^+.$$

Proof. Simply substitute (5.1) into (5.2) and calculate the integral. □

Thus we can employ the "energy defect"

$$\delta := \left|1 - \frac{E^+(l_1) - E^-(l_2)}{\beta_0^+}\right|,$$

to measure the error in our numerical approximation.

Before describing our results, we recall that k^+ and k^- are the wavenumbers in the upper and lower media, respectively, while α is the x-component of the incident radiation and ε measures the height/slope of our profile $y = g(x) = \varepsilon f(x)$ (which is always chosen $d = 2\pi$-periodic). In the first six examples in this section we have chosen $\alpha = 0$ (so that waves are normally incident) and selected the transparent boundaries at $y = a = 1$ and $y = -b = -1$. The numerical parameters are N_x (the number of Fourier modes in the x direction), N_y (the number of Legendre coefficients in the y direction), and N (the number of Taylor coefficients retained in the perturbation expansion).

In the recent work [22], a rigorous numerical error analysis of the TFE method was given for a single layer of dielectric material. We fully expect this analysis to apply directly to the doubly layered model at hand, and that our numerical approach will have very similar behavior, e.g. exponential convergence as N_x, N_y, and N are increased, and the need to increase all of these parameters as k^+ and k^- become large. However, we are also interested in two further questions which we address in the following numerical simulations:

1. As we increase ε so that the profile approaches the artificial boundaries, can we still obtain a reasonable approximation?
2. How does the difference between k^+ and k^- affect our results?

5.2. Numerical results

We now perform a sequence of tests to study the convergence behavior of our algorithm.

1. Convergence study in perturbation order:
   To begin, we fix $d = 2\pi$, $\varepsilon = 0.1$, $N_x = 40$, $N_y = 80$, $f(x) = \cos(x)$, $a = 1$, $b = -1$, and vary $N = 0,\ldots,55$ for five choices of the wavenumbers $k^{\pm}$:

$$(k^+, k^-) = (2.5, 1.25), \quad (k^+, k^-) = (12.5, 6.25), \quad (k^+, k^-) = (25.5, 12.75),$$
$$(k^+, k^-) = (51.5, 25.75), \quad (k^+, k^-) = (102.5, 51.25). \tag{5.3}$$

   The results are displayed in Fig. 2. Clearly, as anticipated, we notice exponential convergence as N is refined. We point out that larger values of the wavenumbers require much larger choices for N, and, furthermore, as we fixed the x and y dis-

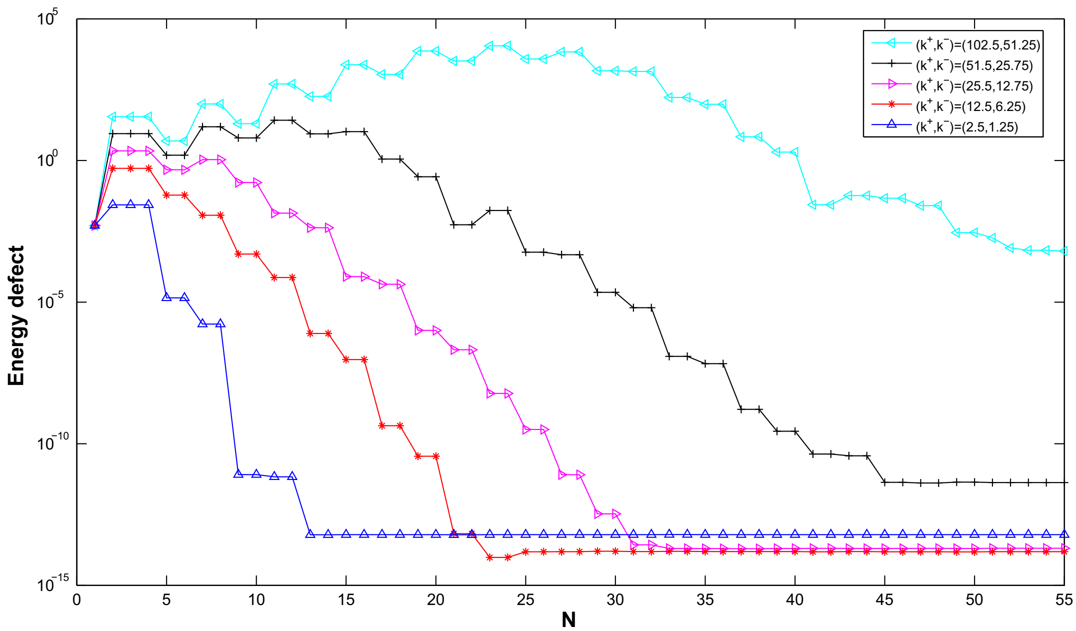

Fig. 2. Energy defect versus perturbation order N.

cretizations at $N_x = 40$ and $N_y = 80$, respectively, the case $(k^+, k^-) = (102.5, 51.25)$ is under-resolved and we can only achieve an error of 10^{-3}.

2. Convergence study in vertical discretization:
We now fix $d = 2\pi$, $\varepsilon = 0.1$, $N_x = 20$, $N = 20$, $f(x) = \cos(x)$, $a = 1$, $b = -1$, and vary $N_y = 1, \ldots, 40$ for the five choices of $k^\pm$ in (5.3). We display the results in Fig. 3. Once again, we notice exponential convergence as N_y is refined, and larger values of the wavenumbers require much larger choices for N_y. Once again, the calculation is under-resolved at $(k^+, k^-) = (102.5, 51.25)$ so that we can only realize an error of 10^{-2} and is thus omitted.
3. Convergence study in horizontal discretization:
We fix $d = 2\pi$, $\varepsilon = 0.1$, $N_y = 80$, $N = 20$, $f(x) = \cos(x)$, $a = 1$, $b = -1$, and vary $N_x = 1, \ldots, 40$ for the first four choices of $k^\pm$ in (5.3). We display the results in Fig. 4. Exponential convergence is once again observed, though for the two larger choices of wavenumber the under-resolution is particularly strong in this calculation.
4. Convergence study for deformations near the artificial boundary:
We now investigate the behavior of our algorithm as the sharp interface and artificial boundary are brought close together. This can, of course, be achieved either by increasing ε, decreasing a (or b) or a combination of both. To fix upon an example we set $d = 2\pi$, $f(x) = \cos(x)$, $N_x = 20$, and $N_y = 40$. We investigate five configurations:
$$(k^+, k^-, N) = (2.5, 1.25, 30), \quad (k^+, k^-, N) = (2.5, 1.25, 50), \quad (k^+, k^-, N) = (12.5, 6.25, 30),$$
$$(k^+, k^-, N) = (12.5, 6.25, 80), \quad (k^+, k^-, N) = (12.5, 6.25, 200),$$
and, letting $\varepsilon = 0.1, 0.2, \ldots, 0.9$, we display the results in Fig. 5.
First, from the previous sections, we observe that parameters $(N_x, N_y, N) = (20, 40, 30)$ are sufficiently large to obtain a high accuracy approximation both for the cases $(k^+, k^-) = (2.5, 1.25)$ and $(k^+, k^-) = (12.5, 5.25)$. Fig. 5 shows that when we let the height of the profile approach the artificial boundaries, the error is only determined by the parameters (k^+, k^-). To achieve the same relative error, for small (k^+, k^-) one can allow the artificial boundaries to be located quite close to the profile. Here Padé approximation (see Remark 4.1) was used to access this region of extended analyticity so that configurations which are large deformations of the base geometry can be simulated [1].
5. Convergence study as wavenumber is varied:
We investigate the effects of varying the ratio of the wavenumber parameters k^-/k^+ in our numerical scheme. We fix $d = 2\pi$, $f(x) = \cos(x)$, $N_x = 40$, $N_y = 80$, $N = 30$, $\varepsilon = 0.1$, $k^+ = 2.5$, and vary k^-.
From Table 1, we can see that the difference between k^+ and k^- has almost no effect on the error if we choose parameters N_x, N_y, and N large enough.
6. Convergence study as energy defect is fixed:
We fix $d = 2\pi$, $f(x) = \cos(x)$, $\varepsilon = 0.1$, and aim to find the smallest set of resolution parameters (N, N_x, N_y) for a range of wavenumber pairs (k^+, k^-) such that an energy defect smaller than 10^{-6} is achieved. The result is listed in Table 2. We observe that only a moderately number of modes/iterations, which grow linearly as the wavenumber increases, are needed to obtain an accuracy of 10^{-6}.

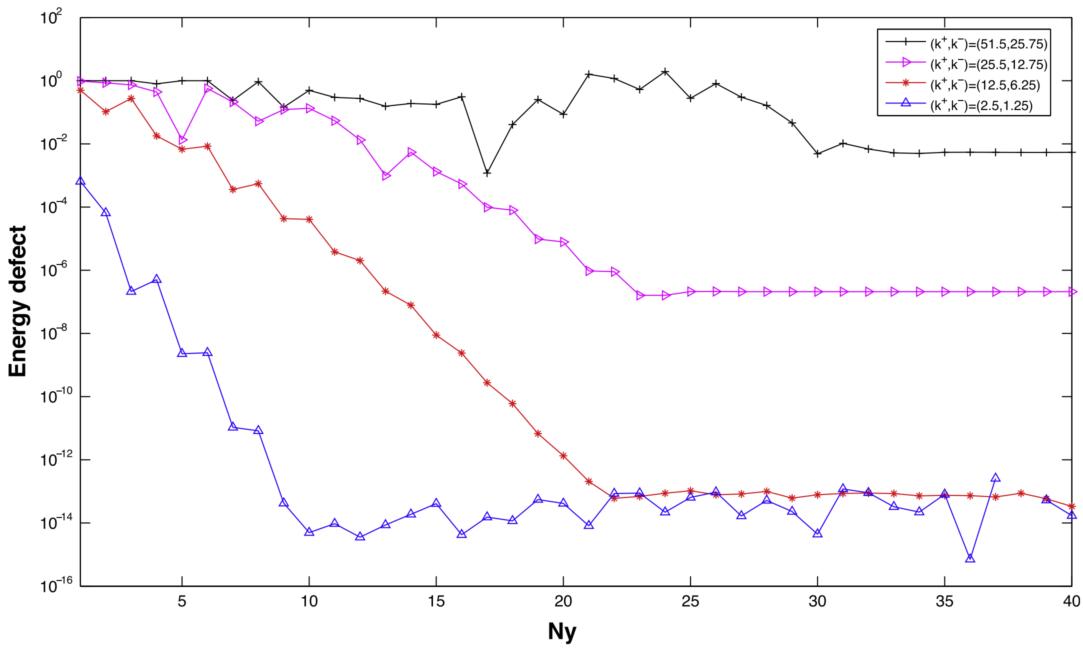

Fig. 3. Energy defect versus vertical discretization N_y.

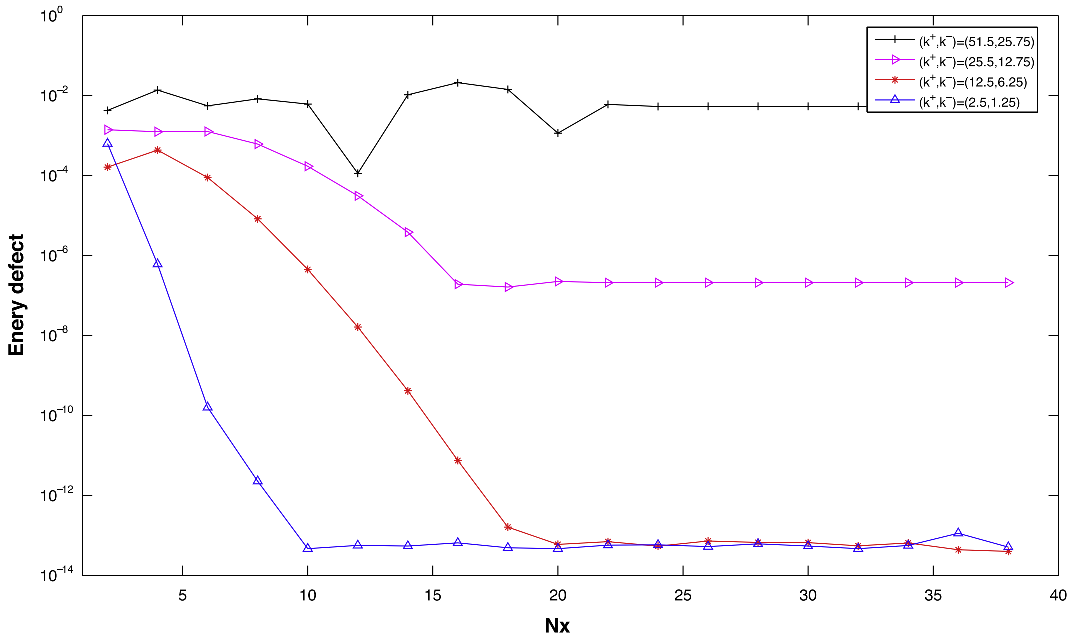

Fig. 4. Energy defect versus horizontal discretization N_x.

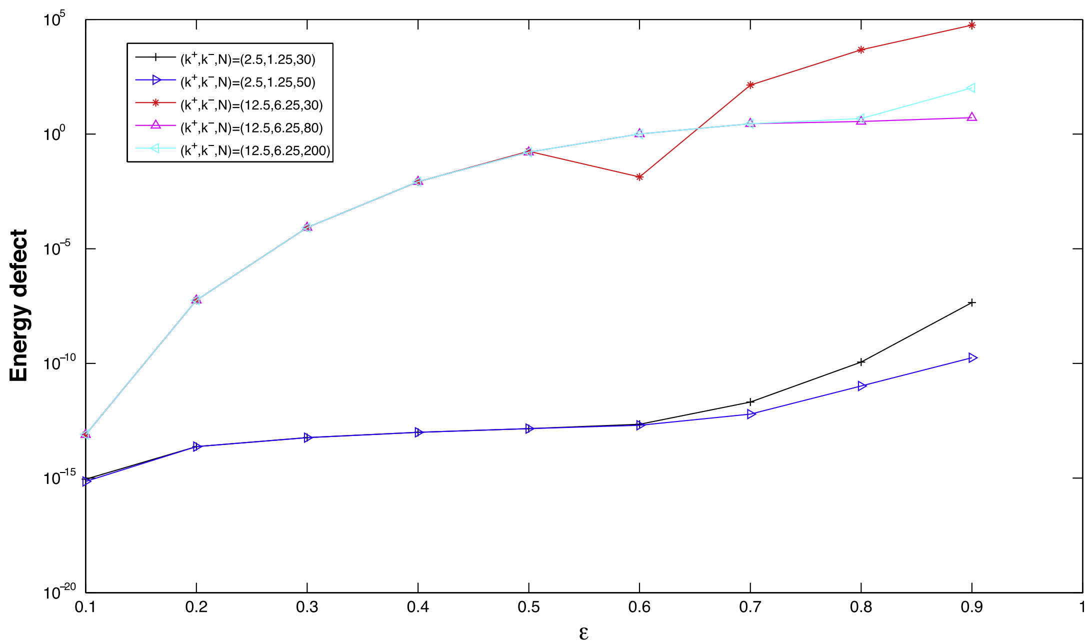

Fig. 5. Energy defect versus ε.

7. Convergence study as incident wave angle is varied:
   For our final study, we investigate the effects of varying the incident wave angle parameter $\cos\theta = \alpha/k^+$ in our numerical scheme. When $\alpha = 0$, it means the wave is normally incident $\left(\theta = \frac{\pi}{2}\right)$. We fix $d = 2\pi$, $f(x) = \cos(x)$, $N_x = 10$, $N_y = 15$, $N = 12$, $\varepsilon = 0.1$, $k^+ = 12.5$, $k^- = 6.25$ and vary α. We observe from Table 2 that $N_x = 10$, $N_y = 15$, $N = 12$ are the smallest numbers to achieve an accuracy of 10^{-6} when $(k^+, k^-, \alpha) = (12.5, 6.25, 0)$. We observe from Table 3 that different α and k^+ have very little effect on the accuracy for a fixed set of parameters N_x, N_y, and N.

Table 1
Energy defect versus wavenumber ratio k^-/k^+.

k^-/k^+	Energy defect	k^-/k^+	Energy defect
0/20	$1.068656274583191 \times 10^{-12}$	10/20	$5.115907697472721 \times 10^{-14}$
1/20	$5.464073637995171 \times 10^{-13}$	11/20	$2.842170943040401 \times 10^{-15}$
2/20	$6.931344387339777 \times 10^{-13}$	12/20	$8.792966355031240 \times 10^{-14}$
3/20	$7.194245199571014 \times 10^{-13}$	13/20	$1.820765760385257 \times 10^{-13}$
4/20	$1.673328142715036 \times 10^{-13}$	14/20	$2.952305067083216 \times 10^{-13}$
5/20	$3.371525281181676 \times 10^{-13}$	15/20	$1.813660333027656 \times 10^{-13}$
6/20	$8.196110456992755 \times 10^{-13}$	16/20	$3.307576434963266 \times 10^{-13}$
7/20	$1.231015289704374 \times 10^{-13}$	17/20	$3.364419853824074 \times 10^{-13}$
8/20	$8.864020628607250 \times 10^{-14}$	18/20	$4.991562718714704 \times 10^{-14}$
9/20	$1.353583911622991 \times 10^{-13}$	19/20	$7.744915819785092 \times 10^{-14}$

Table 2
Smallest (N,N_x,N_y) for (k^+,k^-) to achieve an error of 10^{-6}.

(k^+,k^-)	N	N_x	N_y
(2.5,1.25)	7	6	7
(12.5,6.25)	12	10	15
(25.5,12,75)	20	18	24
(51.5,25.75)	26	26	42
(85.5,42.75)	50	38	63
(105.5,52.75)	60	60	74

Table 3
Energy defect versus incident wave angle α/k^+.

α/k^+	Energy defect	α/k^+	Energy defect
0/10	$5.186341816312279 \times 10^{-6}$	5/10	$2.292137464521894 \times 10^{-5}$
1/10	$1.432592737851698 \times 10^{-5}$	6/10	$7.991322704206624 \times 10^{-6}$
2/10	$9.598113105472218 \times 10^{-6}$	7/10	$6.234791904884309 \times 10^{-6}$
3/10	$7.528997959674400 \times 10^{-6}$	8/10	$3.751204664833842 \times 10^{-6}$
4/10	$1.334178326434116 \times 10^{-5}$	9/10	$9.947091869799839 \times 10^{-7}$

5.3. Concluding remarks

We constructed and implemented a boundary perturbation method for the scattering of electromagnetic waves by doubly layered periodic dielectric media. The method is based on three essential steps: (i) a domain flattening through a change of variable; (ii) a recursion by boundary perturbation; and (iii) an efficient and accurate Legendre–Galerkin method for solving the one-dimensional Helmholtz equation with piecewise constant wavenumbers. The resulting algorithm is shown to be very efficient and stable for a range of small to moderate wavenumbers. On the other hand, our method is not specially designed for the technologically important high-frequency case (reflected in our equations with large values of k). While not beyond the scope of our method, such a simulation would require a very fine discretization of the problem domain resulting in an enormous count of degrees of freedom.

While we have only considered the two-dimensional doubly layered dielectric media, it is expected that the method can be extended to two-dimensional multi-layered periodic media, as well as three-dimensional Maxwell's equations with doubly periodic multi-layered media.

Acknowledgment

The work of Y.H. and J.S. is partially supported by NSF DMS-0915066 and AFOSR FA9550-08-1-0416, while the work of D.P.N. is partially supported by NSF DMS-0810958 and DOE DE-SC0001549.

References

[1] G.A. Baker Jr., P. Graves-Morris, Padé Approximants, Second ed., Cambridge University Press, Cambridge, 1996.
[2] C.M. Bender, S.A. Orszag, Advanced Mathematical Methods for Scientists and Engineers, McGraw-Hill Book Co., New York, 1978. International Series in Pure and Applied Mathematics.
[3] O.P. Bruno, F. Reitich, Numerical solution of diffraction problems: a method of variation of boundaries, J. Opt. Soc. Am. A 10 (6) (1993) 1168–1175.
[4] O.P. Bruno, F. Reitich, Numerical solution of diffraction problems: A method of variation of boundaries. II. Finitely conducting gratings, Padé approximants, and singularities, J. Opt. Soc. Am. A 10 (11) (1993) 2307–2316.
[5] O.P. Bruno, F. Reitich, Numerical solution of diffraction problems: a method of variation of boundaries. III. Doubly periodic gratings, J. Opt. Soc. Am. A 10 (12) (1993) 2551–2562.
[6] D. Colton, R. Kress, Inverse Acoustic and Electromagnetic Scattering Theory, second ed., Springer-Verlag, Berlin, 1998.
[7] P.G. Dinesen, J.S. Hesthaven, Fast and accurate modeling of waveguide grating couplers, J. Opt. Soc. Am. A 17 (9) (2000) 1565–1572.
[8] P.G. Dinesen, J.S. Hesthaven, Fast and accurate modeling of waveguide grating couplers. ii. The three-dimensional vectorial case, J. Opt. Soc. Am. A 18 (11) (2001) 2876–2885.
[9] Q. Fang, D. Nicholls, J. Shen, A stable, high-order method for two-dimensional bounded-obstacle scattering, J. Comput. Phys. 224 (2007) 1145–1169.
[10] L. Greengard, V. Rokhlin, A fast algorithm for particle simulations, J. Comput. Phys. 73 (2) (1987) 325–348.
[11] D.M. Milder, An improved formalism for rough-surface scattering of acoustic and electromagnetic waves, in: Proceedings of SPIE – The International Society for Optical Engineering (San Diego, 1991), vol. 1558, Bellingham, WA, 1991, pp. 213–221.
[12] D.M. Milder, An improved formalism for wave scattering from rough surfaces, J. Acoust. Soc. Am. 89 (2) (1991) 529–541.
[13] D.M. Milder, An improved formalism for electromagnetic scattering from a perfectly conducting rough surface, Radio Sci. 31 (6) (1996) 1369–1376.
[14] D.M. Milder, Role of the admittance operator in rough-surface scattering, J. Acoust. Soc. Am. 100 (2) (1996) 759–768.
[15] D.M. Milder, H.T. Sharp, Efficient computation of rough surface scattering, in: Mathematical and Numerical Aspects of Wave Propagation Phenomena (Strasbourg), SIAM, Philadelphia, PA, 1991, pp. 314–322.
[16] D.M. Milder, H.T. Sharp, An improved formalism for rough surface scattering. ii: Numerical trials in three dimensions, J. Acoust. Soc. Am. 91 (5) (1992) 2620–2626.
[17] M.-S. Min, T.-W. Lee, P.F. Fischer, S.K. Gray, Fourier spectral simulations and Gegenbauer reconstructions for electromagnetic waves in the presence of a metal nanoparticle, J. Comput. Phys. 213 (2) (2006) 730–747.
[18] D. Nicholls, J. Shen, A stable, high-order method for two-dimensional bounded-obstacle scattering, SIAM J. Sci. Comput. 28 (2006) 1398–1419.
[19] D.P. Nicholls, F. Reitich, A new approach to analyticity of Dirichlet–Neumann operators, Proc. Roy. Soc. Edinburgh Ser. A 131 (6) (2001) 1411–1433.
[20] D.P. Nicholls, F. Reitich, Stability of high-order perturbative methods for the computation of Dirichlet–Neumann operators, J. Comput. Phys. 170 (1) (2001) 276–298.
[21] D.P. Nicholls, F. Reitich, Analytic continuation of Dirichlet–Neumann operators, Numer. Math. 94 (1) (2003) 107–146.
[22] D.P. Nicholls, J. Shen, A rigorous numerical analysis of the transformed field expansion method, SIAM J. Numer. Anal. 47 (4) (2009) 2708–2734.
[23] R. Petit (Ed.), Electromagnetic Theory of Gratings, Springer-Verlag, Berlin, 1980.
[24] F. Reitich, K. Tamma, State-of-the-art, trends, and directions in computational electromagnetics, CMES Comput. Model. Eng. Sci. 5 (4) (2004) 287–294.
[25] J. Shen, Efficient spectral-Galerkin method. I. Direct solvers of second- and fourth-order equations using Legendre polynomials, SIAM J. Sci. Comput. 15 (6) (1994) 1489–1505.
[26] J. Shen, T. Tang, Spectral and high-order methods with applications, Mathematics Monograph Series, vol. 3, Science Press, Beijing, 2006.
[27] J. Shen, T. Tang, L.-L. Wang, Spectral methods: algorithms, analysis and applications, Springer Series in Computational Mathematics, vol. 41, Springer, 2011.
[28] J. Shen, L.-L. Wang, Analysis of a spectral-Galerkin approximation to the Helmholtz equation in exterior domains, SIAM J. Numer. Anal. 45 (2007) 1954–1978.
[29] L. Tsang, J.A. Kong, R.T. Shin, Theory of Microwave Remote Sensing, Wiley Series in Remote Sensing, Wiley-Interscience, New York, 1985.
[30] L.C. Wilcox, P.G. Dinesen, J.S. Hesthaven, Fast and accurate boundary variation method for multilayered diffraction optics, J. Opt. Soc. Am. A 21 (5) (2004) 757–769.